Workshop on Visualisation in Environmental Sciences (EnvirVis) (2016)
A. Middel, K. Rink, and D. Zeckzer (Editors)

Short Paper

Visualizing Malaria Spread Under Climate Variability

X. Liang[1], R. Aggarwal[1], A. Cherif[2], A. Gumel[2], G. Mascaro[3] and R. Maciejewski[1]

[1]School of Computing, Informatics & Decision Systems Engineering, Arizona State University, U.S.A.
[2]School of Mathematical & Statistical Sciences, Arizona State University, U.S.A.
[3]School of Sustainable Engineering & the Built Environment, Arizona State University, U.S.A.

Abstract

In order to better control and prevent the infectious diseases, measures of vulnerability and risk to increased infectious disease outbreaks have been explored. Research investigating possible links between variations in climate and transmission of infectious diseases has led to a variety of predictive models for estimating the future impact of infectious disease under projected climate change. Underlying all of these approaches is the connection of multiple data sources and the need for computational models that can capture the spatio-temporal dynamics of emerging infectious diseases and climate variability, especially as the impact of climate variability on the land surface is becoming increasingly critical in predicting the geo-temporal evolution of infectious disease outbreaks. This paper presents an initial visualization prototype that combines data from population and climate simulations as inputs to a patch-based mosquito spread model for analyzing potential disease spread vectors and their relationship to climate variability.

Categories and Subject Descriptors (according to ACM CCS): I.3.8 [Computer Graphics]: Applications—

1. Introduction

As the world's urban population increases over the next generation [Pro12], the coupled effects of population growth and climatic stressors may lead to unprecedented disasters [VMG*10] [CKR*14]. Current and future climate variability is expected to significantly impact ecosystems, water, energy and food security, as well as human health [PAB*14]. A critical impacted area of human health is that of vector-borne infectious diseases. For example, the recent increases in temperature and rainfall in Kenya have corresponded to upsurges in malaria epidemics in the highlands [UND-PUB12], increases in leptospirosis were documented in Brazil after severe flooding [KRD*99], and simulations of drought amplification has suggested increased pathways for West Nile transmission in the United States [Eps01]. What this means is that as long-term incremental climatic shifts occur, the population must learn to adapt to emerging patterns of infectious disease outbreaks.

In order to better control and prevent the infectious diseases, measures of vulnerability and risk to increased infectious disease outbreaks need to be explored. Research investigating possible links between variations in climate and transmission of infectious diseases has led to a variety of predictive models (statistical, process and landscape based) for estimating the future impact of infectious disease under projected climate change [PEBB96] [GN01]. Statistical models such as CLIMEX [Sut98, Sut01] and the Malaria-Potential-Occurrence Zone method [ML95] map the geographical distribution of vector species and relationships to climate change using estimates on minimum and maximum temperatures for parasite development. Process based models such as MIASMA [ML95] and MARA/ARMA [HEM*02] link global climate models (GCMs) and transmission rates of mosquitos to identify the effects of temperature increases on the vectors of infection, and landscape based models (e.g., [RRSH02]) utilize satellite based imagery to estimate disease vectors and risk based on prevalence of water and vegetation. Underlying all of these approaches is the connection of multiple data sources and the need for computational models that can capture the spatio-temporal dynamics of emerging infectious diseases and climate variability, especially as the impact of climate variability on the land surface is becoming increasingly critical in predicting the geo-temporal evolution of infectious disease outbreaks.

Despite recent progress, there is still a need for the development of reliable modeling and visualization frameworks for integrating climate simulations and infectious disease models. In this paper, we present an initial prototype visualization system for exploring a malaria transmission model with climate variable inputs. Here, we focus on simultaneously exploring precipitation and temperature as key boundary variables for mosquito growth rates. We discuss the need to intelligently composite data from a variety of sources, both measured and simulated, as well as speculate on potential design futures for exploring cascading uncertainty between models of climate and disease spread.

DOI: 10.2312/envirvis.20161104

2. Background And Related Work

A myriad of new tools and algorithms have been developed to help public health professionals analyze and visualize the complex data used in infectious disease control, and visual analytical tools are becoming more commonplace in the study of disease spread. Carroll et al. [CAD*14] systematically review many disease visualization tools in the context of users' practical needs and preferences and identify map views as one of the basic and essential needs of users. Besides the static map views, a variety of extensions have been developed. For example, Deodhar et al. [DCW*15] employ time-varying heat maps and graphical plots to view the trends in the disease dynamics. Balcan et al. [BCG*09] employs gravity models in the epidemic transmission from regions to regions and visualizes transmission as a tree-structure graph. Guo [Guo07] proposed a new graph partitioning method to segment disease network graphs into several spatially contiguous subgraphs and reorder them to present the spatial interaction patterns.

Along with geographical representations, a typical visual analytic tool for scenario modeling also involves elements such as line charts or parallel coordinates through coordinated multiple views. For example, work by Maciejewski et al. [MLR*11] presents a visual analytics toolkit called PanViz for analyzing the effect of decision measures implemented during a simulated pandemic influenza scenario. Waser et al. [WFR*10] employs linking and brushing in the metaphor of time frames to enable comparative analysis of visual analysis within different parameters in the flooding models. Bryan et al. [BWMM15] developed a novel visual analytics interface which contains line charts, heat maps, star coordinates and other techniques for predictive simulations and analysis, and Afzal et al. [AME11] utilized a spatiotemporal view where users can interactively utilize mitigative response measures and observe the impact of their decision over time. Based on an analysis of previous work, our prototype implementation focuses on a geographical view with linked time series components. While the visual methods presented are standard, this paper presents an initial example of linking together multi-source data (climate and population) as inputs for a disease-spread model.

3. System Design

Our prototype system consists of a data modeling and collection component and a visual analysis component. In this section we provide a brief overview of the data collection and integration, introduce the epidemic model being used and describe the visualization components of the system.

3.1. Data Modeling

To simulate and explore the relationship between climate variability and transmission of mosquito borne diseases, we first need to provide a model with a set of initial conditions. We use the historical population data as the input for the initial amounts of potential human hosts, the historical temperature and precipitation data as the descriptors of climate variability (which future work will replace with a downscaled ensemble of climate simulations for predictive analysis), and an epidemic model of malaria transmission. Patches in the transmission model are simplified as geographical rectangles in a region.

Population data is collected from Gridded Population of the World (GPW) v3 [CfIESINC05] from the Socioeconomic Data and Applications Center (SEDAC), Columbia University, which contains the estimations of global population density for 1990, 1995 and 2000 [LLM*15]. As the initial amount of human hosts, we use the population data in 2000 as our test data. For computational reasons, we aggregate population to the regions of 5° by 5°.

Climatic factors, such as temperature, humidity, and rainfall, are known to significantly affect the incidence of vector-borne diseases [AGP15]. Extreme weather conditions including high temperature and heavy rainfall generally induce a negative impact on the survival vectors [AGP15], especially for mosquitoes. We collected monthly air temperature and precipitation data from the Climate Research Unit of the University of East Anglia. As input to the model, each patch uses the average precipitation and temperature value of all pixels contained within a patch. Future work will explore downscaling methods for increased temporal and spatial resolutions to improve the model efficacy.

The epidemic model used in our study is based on a meta-population mathematical model for the transmission dynamics of malaria in a community consisting of multiple patches, which takes into account the effect of temperature (air and water) and precipitation variability on the hosts and vectors [AGP15]. The total host population at time t for each patch i, denoted by $N_H^{(i)}(t)$, and is split into four epidemiological states, namely mutually-exclusive susceptible $S_H^{(i)}(t)$, exposed (with no clinical symptoms of malaria) $E_H^{(i)}(t)$, infectious $I_H^{(i)}(t)$ and recovered individuals $R_H^{(i)}(t)$, where $N_H^{(i)}(t) = S_H^{(i)}(t) + E_H^{(i)}(t) + I_H^{(i)}(t) + R_H^{(i)}(t)$. Similarly, the total population for vectors at time t for each patch i, denoted by $N_V^{(i)}(t)$, is subdivided into three compartments where $L_V^{(i)}$ denotes the immature mosquitoes (eggs, larvae and pupae), adult mosquitoes $S_V^{(i)}(t)$, and infectious mosquitoes $I_V^{(i)}(t)$. Hence, $N_V^{(i)}(t) = L_V^{(i)}(t) + S_V^{(i)}(t) + I_V^{(i)}(t)$. The equations for the patch model considered in this study take the simplified form of the deterministic system of non-linear differential equations given in [AGP15] within the multi-patch framework. Though there is a large number of parameters in this model, we primarily use the values suggested in Agusto et al. [AGP15] and only tweak the climatic variables based on historical data. Related computations for solving the differential equations on the web-based system is supported by Parallel Javascript library [Sav16] and Numeric Javascript library [Loi16].

3.2. Visual Analytical View

Our prototype system consists of two visualization elements: line charts and map views. Line charts are used for representing the change of each model variable over the time. Map views are used for showing the spatial distribution of disease transmission, temperature and precipitation, as shown in Figure 1. In the geographic views, each patch is a semi-transparent rectangle. In the largest map, patches in red denote higher volumes of infectious humans and patches in green denote the lower volumes. Gray patches represent regions where population data is unavailable, and future work

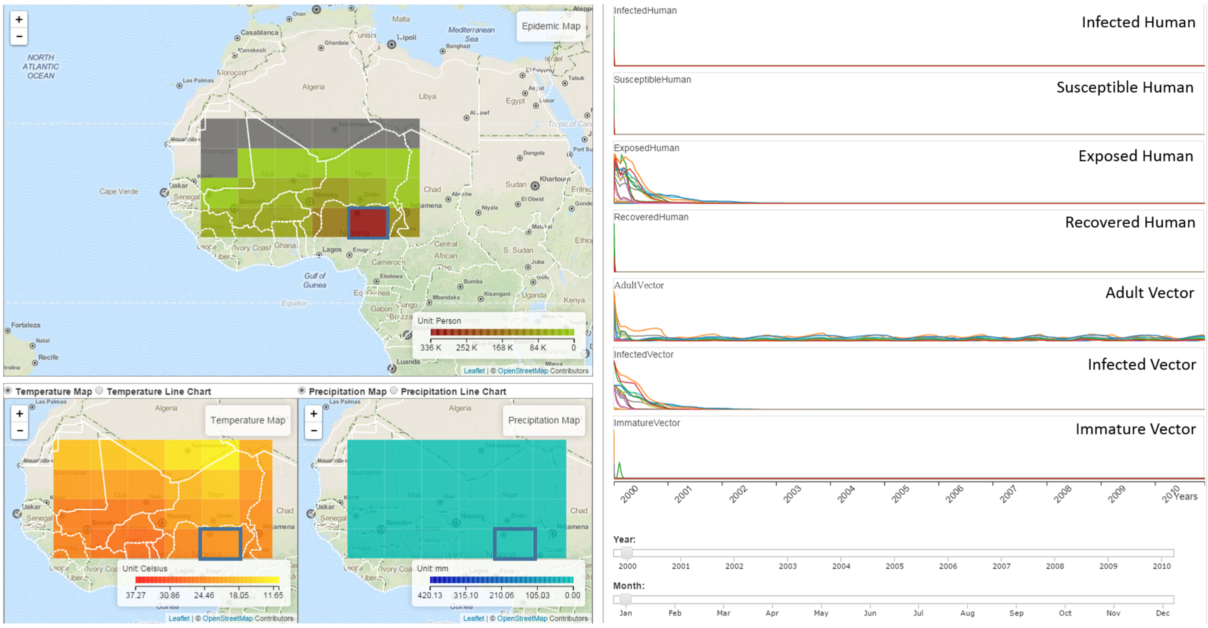

Figure 1: *Overview of the default system. The top left map shows the spatial distribution of infected humans. The patch highlighted by the blue rectangle is identified as the center of disease and population diffusion. The lower left two maps show the distribution of temperature and precipitation which can also be switched to line chart views showing their temporal changes. The right line charts show the changing amount of seven states in host and vectors by the time. The lower right sliders are used for changing the time by months or by years.*

will explore methods for automatically estimating population from satellite imagery. For the other two maps, the left map shows the temperature distribution with orange representing higher temperatures and yellow representing lower temperatures. The right map shows the precipitation with darker blue being larger amounts of precipitation. To see the temporal trend of the temperature or precipitation, users may click the radio button above the two maps and switch between the map view and line chart view.

The right part of our interface, Figure 1, consists of seven line charts each showing the host and vector states over time (these are the states previously defined in Section 3.1). The x-axis represents time and the y-axis represents the amount of the host or vector in that state. Each line in the line charts represents a patch and is distinguished by the color. From top to bottom, these states are infectious host, susceptible host, exposed host, recovered host, adult vector, infected vector and immature vector. Despite the visual clutter in the line charts, users can mouse over the patch on the map to highlight the corresponding line.

4. Case Study

Our current prototype focuses on the West Africa region near the Niger basin where temperature and precipitation patterns are regularly affected by latitude and the West African monsoon. What is of interest is exploring how changes in climate will impact the resultant amount of malaria cases. In the epidemic model, the influence from the temperature are directly projected onto the natural mortality rate of immature mosquitoes, egg deposition rate and maturation rate, which will further affect the amount of infected vectors and the infectious host. Therefore, it is reasonable to expect that the change of adult and immature vectors, even for the infected host, may follow the change of temperature or precipitation. Also, due to the mobility of the population among patches, which is also considered in the epidemic model, we can make a bold presumption that the infectious host or infected vectors will also diffuse or transmit among patches. To validate the above assumptions, the model visualization is explored by modeling experts.

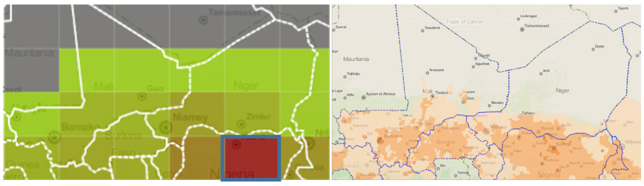

Figure 2: *The left map shows the distribution of infectious host and the right map shows the population distribution in higher resolution. Patch 23 is highlighted with the blue rectangle in the left map. It is easy to see the similar radial diffusion on both maps.*

4.1. Parameter Settings

In this model, humans and mosquitoes are considered as the disease host and vectors respectively. All parameters, except the initial total of hosts, vectors, initial infectious hosts, infected vectors, temperature and precipitation, are fixed using the values of Agusto et al. [AGP15]. The amount of vectors is proportional to the mag-

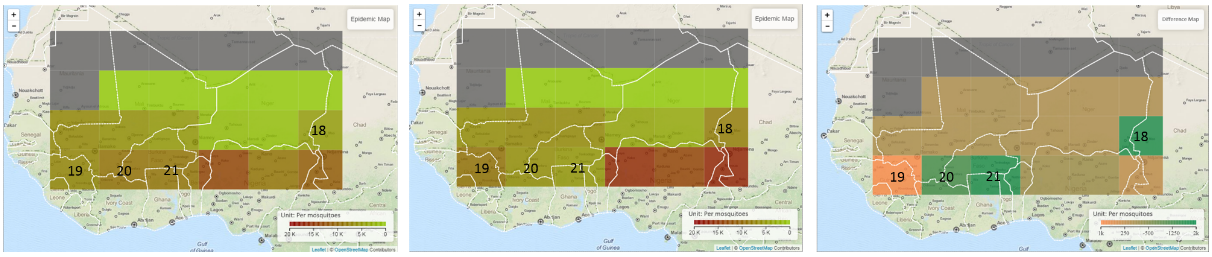

Figure 3: *Difference maps for the infected mosquitoes in March 2000 among simulations with historical temperature (left),* 2 °C *higher temperature (middle), and their differences (right). The color in the right map from orange to green represents the changes from the growth of 1000 mosquitoes to the reduction of 2000 mosquitoes between the two scenarios. Patch 18, 19, 20, and 21 are highlighted by the numbers.*

nitude of the total hosts and can be modified as more mosquito collection reports are provided. The amount of initial infectious hosts and infected mosquitoes are set as ten percent of the total amount of host and vector separately. The West Africa region is uniformly split into 24 patches and they are numbered from 1 to 24 for convenience from left to right and from top to bottom. During the computation, temperature and precipitation are loaded from the collected historical data directly. The step size during the integration of the differential equations is taken as 10^{-6}.

4.2. Simulation Results And Analysis

Figure 1 shows the default visualization at the beginning of the simulation. The epidemic map on the top-left shows the distribution of initial infectious humans. Because this value is assigned proportionally to the total human amount, we can see its distribution is similar to a radial diffusion within the center at patch 23. A comparison between the actual population distribution and infectious human distribution is shown in Figure 2.

To further study the relationship between climate variability and disease transmission, users can change the time slice by dragging the slide bars. It is evident in the line chart of infectious humans, which is the top line chart in Figure 1, that the infection will eventually subside. Besides the amount of infectious humans, the amount of susceptible humans and recovered humans also show a similar pattern. We can see that the amount of exposed humans reduces gradually and goes to zero after two years approximately. What is interesting is that adult mosquitoes only provide the basis population for the vector and only the infected mosquitoes have the ability to transmit the virus to humans or other mosquitoes. As we can see, the line chart of the infected vector in Figure 1 generally shows a negative growth rate, which means the chance of the transmission of the virus becomes less over time from the initial outbreak.

5. Conclusions and Future Work

While our prototype system provides a method for linking multi-source data with disease transmission models, the goal of this project is to develop a way to explore the impact of future climate variability. Thus, future work will explore the creation of disease risk maps using an ensemble of climate simulations as input to the model. As an explorative trial, Figure 3 shows a simple first pass difference map where the user simply compares what happens to disease transmission if the average temperature increases by 2 °C. The left two maps show the distribution of infected mosquitoes with historical temperature and 2 °C higher temperature. In the rightmost map, we can see more infected mosquitoes emerging in some areas such as patch 19 and less infected vectors in other areas such as patch 18, 20 and 21. What is difficult is trying to assess the overall "risk" of disease in an area. We can indicate that given a change in temperature, an area will see more (or less) mosquitoes, which are the primary vector for disease spread. However, quantifying this into a probability measure is very difficult.

With respect to future designs, the ultimate goal is to create a visualization that is capable of providing insights into the interaction between the spatial heterogeneity, climate dynamics on gonotrophic process, larva and plasmodium development and vector survivability, and spatial disease dynamics (e.g., epidemic size, prevalence, incidence and probability of epidemics). In the current preliminary work, we demonstrate that different geographic regions will see the mosquito vector vary. As regions become too hot, mosquitoes die off, but regions that were previously too cold for mosquitoes to thrive now can become vulnerable. However, population expansion and migration also need to be considered. As such, a visual analytics toolkit for exploring climatic variability and disease spread needs to be able to communicate multiple factors as well as uncertainties underlying both individual model components (models for population, climate and disease) as well as the uncertainty that results due to the coupling of the model. Future work will explore a variety of multivariate visualization techniques coupled with data abstraction to demonstrate changes of the spread vectors and risk as a function of climatic and population variability.

Acknowledgement

Some of the material presented here was supported by the NSF under Grant No. 1350573, in part by the U.S. Department of Homeland Security VACCINE Center under Award Number 2009-ST-061-CI0001, and by the Global Security Initiative at Arizona State University. One of authors (ABG) is grateful to National Institute for Mathematical and Biological Synthesis (NIMBioS) for funding the Working Group on Climate Change and Vector-borne Diseases. NIMBioS is an Institute sponsored by the National Science Foundation, the U.S. Department of Homeland Security, and the U.S. Department of Agriculture through NSF Award #EF-0832858, with additional support from The University of Tennessee, Knoxville.

References

[AGP15] Agusto F., Gumel A. B., Parham P.: Qualitative assessment of the role of temperature variations on malaria transmission dynamics. *Journal of Biological Systems 23*, 04 (2015), 1550030. 2, 3

[AME11] Afzal S., Maciejewski R., Ebert D. S.: Visual analytics decision support environment for epidemic modeling and response evaluation. In *IEEE Conference on Visual Analytics Science and Technology (VAST)* (2011), pp. 191–200. 2

[BCG*09] Balcan D., Colizza V., Gonçalves B., Hu H., Ramasco J. J., Vespignani A.: Multiscale mobility networks and the spatial spreading of infectious diseases. *Proceedings of the National Academy of Sciences 106*, 51 (2009), 21484–21489. 2

[BWMM15] Bryan C., Wu X., Mniszewski S., Ma K.-L.: Integrating predictive analytics into a spatiotemporal epidemic simulation. In *IEEE Conference on Visual Analytics Science and Technology (VAST)* (2015), pp. 17–24. 2

[CAD*14] Carroll L. N., Au A. P., Detwiler L. T., Fu T.-c., Painter I. S., Abernethy N. F.: Visualization and analytics tools for infectious disease epidemiology: A systematic review. *Journal of biomedical informatics 51* (2014), 287–298. 2

[CfIESINC05] Center for International Earth Science Information Network (CIESIN) C. I. d. A. T. C.: Gridded population of the world, version 3 (gpwv3) data collection. http://sedac.ciesin.columbia.edu/gpw/index.jsp, 2005. 2

[CKR*14] Caminade C., Kovats S., Rocklov J., Tompkins A. M., Morse A. P., Colón-González F. J., Stenlund H., Martens P., Lloyd S. J.: Impact of climate change on global malaria distribution. *Proceedings of the National Academy of Sciences 111*, 9 (2014), 3286–3291. 1

[DCW*15] Deodhar S., Chen J., Wilson M., Bisset K., Barrett C., Marathe M.: Epicaster: An integrated web application for situation assessment and forecasting of global epidemics. In *Proceedings of the 6th ACM Conference on Bioinformatics, Computational Biology and Health Informatics* (2015), ACM, pp. 156–165. 2

[Eps01] Epstein P. R.: West nile virus and the climate. *Journal of Urban Health 78*, 2 (2001), 367–371. 1

[GN01] Githeko A. K., Ndegwa W.: Predicting malaria epidemics in the kenyan highlands using climate data: a tool for decision makers. *Global Change and Human Health 2*, 1 (2001), 54–63. 1

[Guo07] Guo D.: Visual analytics of spatial interaction patterns for pandemic decision support. *International Journal of Geographical Information Science 21*, 8 (2007), 859–877. 2

[HEM*02] Hartman J., Ebi K., McConnell K. J., Chan N., Weyant J.: Climate suitability: For stable malaria transmission in zimbabwe under different climate change scenarios. *Global Change and Human Health 3*, 1 (2002), 42–54. 1

[KRD*99] Ko A. I., Reis M. G., Dourado C. M. R., Johnson W. D., Riley L. W., Group S. L. S., et al.: Urban epidemic of severe leptospirosis in brazil. *The Lancet 354*, 9181 (1999), 820–825. 1

[LLM*15] Lei T., Liang X., Mascaro G., Luo W., White D., Westerhoff P., Maciejewski R.: An interactive web-based geovisual analytics tool to explore water scarcity in niger river basin. 2

[Loi16] Loisel S.: Numeric javascript. http://www.numericjs.com/, Februrary 2016. 2

[ML95] Martin P. H., Lefebvre M. G.: Malaria and climate: Sensitivity of malaria potential transmission to climate. *Ambio (Sweden)* (1995). 1

[MLR*11] Maciejewski R., Livengood P., Rudolph S., Collins T. F., Ebert D. S., Brigantic R. T., Corley C. D., Muller G. A., Sanders S. W.: A pandemic influenza modeling and visualization tool. *Journal of Visual Languages & Computing 22*, 4 (2011), 268–278. 2

[PAB*14] Pachauri R. K., Allen M., Barros V., Broome J., Cramer W., Christ R., Church J., Clarke L., Dahe Q., Dasgupta P., et al.: Climate change 2014: Synthesis report. contribution of working groups i, ii and iii to the fifth assessment report of the intergovernmental panel on climate change. 1

[PEBB96] Patz J. A., Epstein P. R., Burke T. A., Balbus J. M.: Global climate change and emerging infectious diseases. *Jama 275*, 3 (1996), 217–223. 1

[Pro12] Programme U. N. D.: *The Sustainable Future We Want*. UNDP in action. 2012. URL: https://books.google.com/books?id=02TqNAEACAAJ. 1

[RRSH02] Rogers D. J., Randolph S. E., Snow R. W., Hay S. I.: Satellite imagery in the study and forecast of malaria. *Nature 415*, 6872 (2002), 710–715. 1

[Sav16] Savitzky A.: Parallel.js. https://adambom.github.io/parallel.js/, Februrary 2016. 2

[Sut98] Sutherst R.: Implications of global change and climate variability for vector-borne diseases: Generic approaches to impact assessments. *International journal for parasitology 28*, 6 (1998), 935–945. 1

[Sut01] Sutherst R. W.: The vulnerability of animal and human health to parasites under global change. *International journal for parasitology 31*, 9 (2001), 933–948. 1

[UNDPUB12] United Nations Development Programme (UNDP) B. f. C. P., (BCPR) R.: *Climate Risk Management for Malaria Control in Kenya: The Case of the Western Highlands*. UNDP in action. New York, NY: UNDP BCPR, 2012. URL: https://books.google.com/books?id=02TqNAEACAAJ. 1

[VMG*10] Vörösmarty C. J., McIntyre P. B., Gessner M. O., Dudgeon D., Prusevich A., Green P., Glidden S., Bunn S. E., Sullivan C. A., Liermann C. R., et al.: Global threats to human water security and river biodiversity. *Nature 467*, 7315 (2010), 555–561. 1

[WFR*10] Waser J., Fuchs R., Ribičić H., Schindler B., Blöschl G., Gröller M. E.: World lines. *IEEE Transactions on Visualization and Computer Graphics 16*, 6 (2010), 1458–1467. 2